HHS Public Access

Author manuscript

Endocr Relat Cancer. Author manuscript; available in PMC 2017 September 06.

Published in final edited form as:

Endocr Relat Cancer. 2015 August ; 22(4): 623–632. doi:10.1530/ERC-15-0058.

Development of pheochromocytoma in ceramide synthase 2 null mice

Woo-Jae Park[1,2,*], **Ori Brenner**[3,*], **Aviram Kogot-Levin**[1,4], **Ann Saada**[4], **Alfred H. Merrill Jr.**[5], **Yael Pewzner-Jung**[1], and **Anthony H. Futerman**[1]

[1]Department of Biological Chemistry, Weizmann Institute of Science, Rehovot 76100, Israel

[2]Department of Biochemistry, School of Medicine, Gachon University, Incheon 406-799, South Korea

[3]Department of Veterinary Resources, Weizmann Institute of Science, Rehovot 76100, Israel

[4]Monique and Jacques Roboh Department of Genetic Research, Department of Genetics and Metabolic Diseases, Hadassah, Hebrew University Medical Center, Jerusalem, Israel

[5]School of Biology and Petit Institute for Bioengineering and Bioscience, Georgia Institute of Technology, Atlanta, Georgia 30332-0230

Abstract

Pheochromocytoma (PCC) and paraganglioma are rare neuroendocrine tumors of the adrenal medulla and sympathetic and parasympathetic paraganglia, for which mutations in ~15 disease-associated genes have been identified. We now document the role of an additional gene in mice, the ceramide synthase 2 (CerS2) gene. CerS2, one of six mammalian CerS, synthesizes ceramides with very-long (C22–C24) acyl chains. The CerS2 null mouse has been well characterized and displays lesions in several organs including the liver, lung and the brain. We now demonstrate that changes in the sphingolipid acyl chain profile of the adrenal gland lead to the generation of adrenal medullar tumors. Histological analyses revealed that about half of the CerS2 null mice developed PCC by ~13 months, and the rest showed signs of medullary hyperplasia. Norepinephrine and normetanephrine levels in the urine were elevated at 7 months of age consistent with the morphological abnormalities found at later ages. Accumulation of ceroid in the X-zone was observed as early as 2 months of age and as a consequence, older mice displayed elevated levels of lysosomal cathepsins, reduced proteasome activity and reduced activity of mitochondrial complex IV by six months of age. Together, these findings implicate an additional pathway that can lead to PCC formation, which involves alterations in the sphingolipid acyl chain length. Analysis of the role of sphingolipids in PCC may lead to further understanding of the mechanism by which PCC develops, and might implicate the sphingolipid pathway as a possible novel therapeutic target for this rare tumor.

Correspondence should be addressed to: Yael Pewzner-Jung, PhD, Department of Biological Chemistry, Weizmann Institute of Science, Rehovot, Israel 76100. yael.pewzner-jung@weizmann.ac.il.

*W.J. Park and O. Brenner contributed equally to this work

Declaration of interest

The authors declare no conflict of interest.

Keywords

Sphingolipid; ceramide; acyl chain length; oxidative stress; ceroid; lipofuscin; pheochromocytoma

Introduction

The adrenal gland contains two distinct hormone-producing zones, the outer adrenal cortex, which produces glucocorticoids and mineralocorticoids, and the adrenal medulla, which is directly innervated from sympathetic nerves and secretes norepinephrine (NE) and epinephrine (E), which participate in the fight-or-flight response (Rosol *et al.* 2001). In mice, particularly in females, a region defined as the X-zone is located between the cortex and the medulla. However, there are significant differences between the X-zone in mice and humans with the X-zone apparent long after birth in mice (Sucheston & Cannon 1968); moreover, in aged mice, accumulation of lipofuscin, also known as aging pigment or ceroid, is detected in the X-zone (Rosol *et al.* 2001; Seehafer & Pearce 2006) and may extend into the medulla (Greaves 2011). Ceroid, a generic name given to lipopigments that accumulate in association with lipid degeneration or lipid excess, accumulates in lysosomes and consists of advanced lipoxidation end-products (ALEs), which harbor biochemical modifications leading to crosslinking of proteins, lipids and carbohydrates. Ceroid accumulation is associated with vitamin E deficiency, and with neurodegenerative diseases such as the neuronal ceroid lipofuscinoses (NCLs), possibly reflecting chronic oxidative stress (Weglicki *et al.* 1968; Seehafer & Pearce 2006; Hayashi 2009). Chronic oxidative stress and ceroid formation have been associated with tumor formation in the adrenal gland, and in particular with pheochromocytoma (PCC) (Pacak 2011). In humans, PCC is a rare tumor of which ~25% of cases are associated with germline mutations, commonly in subunits of succinate dehydrogenase (SDH), which is part of mitochondrial complex II (Kantorovich & Pacak 2010).

We recently generated a ceramide synthase 2 (CerS2) null mouse (Pewzner-Jung *et al.* 2010a) and now document a high incidence of bilateral medullary hyperplasia and PCC in mice older than 13 months of age. CerS2 is one of six mammalian CerS (Levy & Futerman 2010; Park *et al.* 2013), each of which synthesizes ceramide, a key intermediate in the pathway of sphingolipid (SL) biosynthesis (Levy & Futerman 2010; Park *et al.* 2013) and an important signaling lipid (Hannun & Obeid 2008), with acyl chains of different length. The CerS2 null mouse is unable to synthesize very-long chain (VLC) ceramides (C22–C24-ceramides), and as a result, the ceramide and SL profile is altered such that the mice contain no VLC-SLs but rather contain elevated levels of long chain (LC) SLs, and in some cases, elevated levels of the CerS substrate, sphinganine (Pewzner-Jung *et al.* 2010a; Ben-David *et al.* 2011). These mice develop lesions in several organs including the liver (progressive hepatopathy), lung (emphysema and chronic inflammation) and brain (bilateral and symmetrical demyelination) (Pewzner-Jung *et al.* 2010b; Ben-David *et al.* 2011; Petrache *et al.* 2013), and as we now report, in the adrenal gland. The mechanism of PCC formation in CerS2 null mice may be related to mitochondrial dysfunction due to complex IV deficiency, as has been observed in hepatocytes from these mice (Zigdon *et al.* 2013).

Materials and Methods

Materials

N-succinyl-Leu-Leu-Val-Tyr-7-amido-4-methylcoumarin (suc-LLVY-MCA) was from Sigma-Aldrich (St Louis, MO). The antibodies used in this study were anti-CerS2 (Sigma Aldrich, St Louis, MO), anti-cathepsin D, anti-cathepsin L and anti-cathepsin S (Santa Cruz Biotechnology, Santa Cruz, CA), anti-HNE-Michael adducts (Calbiochem, San Diego, CA), anti-glyceraldehyde 3-phosphate dehydrogenase (GAPDH) (Millipore, Temecula, CA) and anti-F4/80 (Biolegend, San Diego, CA).

Generation and maintenance of CerS2 null mice

CerS2 null mice were generated as described (Pewzner-Jung *et al.* 2010a). All mice were treated according to the Animal Care Guidelines of the Weizmann Institute of Science Animal Care Committee and the National Institutes of Health's Guidelines for Animal Care.

Real time polymerase chain reaction

RNA was extracted using the RNeasy Mini Kit (Qiagen, Valencia, CA) and cDNA was generated using the Verso™ cDNA Synthesis Kit (Thermo Scientific, Hudson, NH). Real time polymerase chain reaction (RT-PCR) was performed using a SYBR Green PCR reaction master mix (Finnzyme, Espoo, Finland) and an ABI Prism 7000 Sequence Detection System (Applied Biosystems, Foster City, CA). Primers for cathepsin were from Vitner *et al.* 2010.

Macroscopic and microscopic analyses

Mice were removed for necropsy at various ages. The pathological study was based on 49 mice (30 CerS2 null (15 males and 15 females) and 19 wild type (WT) mice (5 males and 14 females)) aged 2–19.5 months. This group includes 21 mice older than 13.5 months (the youngest age at which PCC was observed), 11 CerS2 null mice (6 females and 5 males) and 10 WT mice (7 females and 3 males). The adrenal gland was freshly excised, weighed, photographed and fixed. Samples for histology were fixed in 10% neutral buffered formalin, processed routinely and stained with hematoxylin and eosin (HE), Nissl, Periodic acid-Schiff (PAS) or Ziehl-Nielsen and Pearl's iron stains. Sections for immunohistochemistry were fixed in 3% paraformaldehyde for 2 days. Paraffin sections (4 μm) were deparaffinized and antigen retrieval was performed using 10 mM citric acid (pH 6.0) prior to blocking in 20% horse serum in phosphate-buffered saline (PBS) containing 0.2% Triton X-100 for 2 h. Antibodies were added overnight at 4°C and a biotinylated secondary antibody was added for 2 h. Sections were processed with an avidin-biotin HRP kit (ABC kit, Vector Laboratories, Burlingame, CA) for 2 h and developed using diaminobenzidine (DAB) (Sigma Aldrich, St Louis, MO).

Electrospray ionization-tandem mass spectrometry

Electrospray ionization tandem mass spectrometry (ESI-MS/MS) was performed using a PE-Sciex API 3000 triple quadrupole mass spectrometer and an ABI 4000 quadrupole-linear ion trap mass spectrometer (Shaner *et al.* 2009; Sullards *et al.* 2011).

Western blotting

The adrenal gland was homogenized with radioimmunoprecipitation assay (RIPA) buffer (50 mM Tris pH7.5, 150 mM NaCl, 1% Nonidet P-40, 0.5% sodium deoxycholate, 0.1% SDS and protease inhibitors) and incubated at 4°C for 30 min. Lysates were centrifuged (10 min, 10,000×g_{av}, 4°C) and protein in the supernatant measured using a BCA Protein Assay Kit (Pierce Chemical Co., Rockford, IL). Fifty micrograms was loaded on 10% SDS-PAGE gels and transferred to a nitrocellulose membrane. Membranes were blocked with 5% bovine serum albumin (BSA) in PBST (PBS, 0.1% Tween-20) and primary and secondary antibodies were applied. Chemiluminescence was performed using a SuperSignal West Pico Chemiluminescent Substrate (Thermo Scientific Inc., Bremen, Germany).

Stress-induced corticosterone secretion

CerS2 null mice were restrained for 30 min using a 50 ml conical tube with the bottom removed (Chen *et al.* 2006). Blood was collected before, 30 min and 60 min after restraint and serum was isolated. Corticosterone levels were measured using a corticosterone ELISA kit (Cayman Chemical, Ann Arbor, MI). Epinephrine, metanephrine, norepinephrine and normetanephrine levels in urine were analyzed by the Bio-Rad HPLC method (Peaston *et al.* 1996).

Biochemical assays

Cathepsin D activity was measured using a Cathepsin D activity assay kit (Biovision, Palo Alto, CA). Activities of mitochondrial respiratory complexes were measured as described (Zigdon *et al.* 2013). For activity of the 20S proteasome (Sitte *et al.* 2000), the adrenal gland was homogenized in lysis buffer (0.25 M sucrose, 25 mM HEPES (pH 7.8), 10 mM $MgCl_2$, 1 mM EDTA, 1 mM dithiothreitol) and centrifuged (10 min, 14,000×g_{av}, 4°C). Five μg of protein from the supernatant was diluted in 100 μl proteolysis buffer (50 mM Tris (pH 7.8), 20 mM KCl, 5 mM MgOAc, 0.5 mM dithiothreitol) and incubated with 200 μM Suc-LLVY-MCA at 37°C for 1 h. The reaction was terminated by adding 1 volume of cold ethanol and measured at 380 nm excitation and 440 nm emission after addition of 0.125 M sodium borate (pH 9.0). Free methylcoumarin (MCA) was used for quantification.

Results

CerS2 is the major CerS transcribed in the adrenal gland (Fig. 1A) and as expected, no CerS2 mRNA was detected in the adrenal gland of CerS2 null mice, in which a small elevation of CerS1 mRNA was detected (Fig. 1A). VLC-ceramides were the major ceramide species in the adrenal gland of WT mice and were significantly reduced in CerS2 null mice, while levels of C16:0 and C18:0-ceramides were elevated (Fig. 1B); as a result, total ceramide levels were elevated ~2-fold, similar to that observed in some other tissues (Ben-David *et al.* 2011; Pewzner-Jung *et al.* 2014). Sphinganine and sphingosine levels were also elevated (Fig. 1B). CerS2 was detected both in the cortex and medulla of WT adrenal glands, although at higher levels in the cortex, but was not detected in CerS2 null mice (Fig. 1C). A similar expression pattern was observed by x-gal staining (which detects the LacZ gene inserted in the first intron of the CerS2 gene in the CerS2 null allele) (Fig. 1D). CerS2 was not detected in the X-zone (Fig. 1C and D).

Ceroid accumulation in CerS2 null mouse adrenal gland

Since CerS2 was the major CerS in the adrenal gland, we examined the effect of ablating CerS2 on adrenal gland pathology. Mild to marked ceroid accumulation was observed in the X-zone of CerS2 null mice as early as 2 months of age, and was often more severe in older mice (Fig. 2A), although no differences were observed between male and female mice. The material accumulated in, and distended the cytoplasm of cells arranged into variably-sized clusters. The clusters were most-commonly concentrated in the X-zone but in some cases were also found in the cortex and in the medulla (Fig. 2A). The ceroid was finely granular, light brown by the HE stain, PAS-positive, acid fast negative for iron (Fig. 2B), and autofluorescent (Fig. 2C), as is typical of ceroid (Greaves 2011). Ceroid-laden cells were F4/80-positive (Fig. 2D) and sometimes multinucleated, consistent with macrophages.

We also examined levels of cathepsins since ceroid is known to affect lysosome function (Keller *et al.* 2004). mRNA levels of a number of cathepsins were significantly elevated (Fig. 3A), as were protein levels of cathepsin D, L and S (Fig. 3B) and activity of cathepsin D (Fig. 3C). Cathepsins D, L and S were localized in ceroid aggregates (Fig. 3D). Proteasome activity, which can be reduced by lipofuscin or ceroid (Sitte *et al.* 2000), was decreased between 2–6 months of age (Fig. 3E).

Mitochondrial dysfunction in CerS2 null mouse adrenal gland

Since ceroid can be formed as a result of oxidative stress (Kurz *et al.* 2007), we analyzed oxidative stress in the adrenal glands of CerS2 null mice. Lipid peroxidation products (identified using the anti-4-hydroxy-2,3-nonenal (HNE)-Michael adducts antibody) co-localized with ceroid aggregates (Fig. 4A), suggesting that chronic oxidative stress may lead to ceroid formation, or vice versa. No difference in the activity of the mitochondrial electron transport chain was detected at 2 months of age (not shown), but a significant reduction in the activities of mitochondrial complexes III and IV was detected in adrenal glands from 6 month-old CerS2 null mice (Fig. 4B), consistent with the notion that mitochondrial dysfunction is secondary to ceroid formation (Terman *et al.* 2006).

CerS2 null mice develop PCC and secrete elevated levels of epinephrine and norepinephrine

Bilateral pheochromocytoma (PCC) was found in 6 out of 11 CerS2 null mice (3 males and 3 females) between the ages of 13–19 months (Fig. 5A). In the remaining 5 CerS2 null mice, medullary hyperplasia (unilateral or bilateral) was observed (Fig. 5B). Microscopic examination of mice with PCC showed marked enlargement of the adrenal gland in medullary tissue of heterogeneous appearance, which at times compressed the cortex into a thin peripheral band (Fig. 6A). The neoplastic cells were of variable cellular and nuclear size, variable cytoplasmic staining (dark blue to clear), variable nuclear to cytoplasmic ratio, and were arranged in irregular nodules (Fig. 6B). The mitotic rate was high (Fig 6B arrows). Clusters of ceroid-laden cells were common throughout the tumor (Fig. 6C, asterisks), as were irregular areas of fibrillar eosinophlic material, consistent with neuronal processes.

Medullary hyperplasia (Mohr 1992) was seen at an earlier age than PCC in the CerS2 null mouse (Fig. 6D). It was present in 3 out of 6 of the 10.5–11 month-old males and in 4 out of

5 of the 12 month-old females. In this group, hyperplasia appeared to be in its early stage and the histologic findings were subtle and in some cases equivocal. By definition, in all cases with hyperplasia, the architecture of the adrenal gland was well-preserved and without significant cortical atrophy (Fig. 6D, E). Paragangliomas were not identified. None of the histologic changes (i.e. PCC or hyperplasia) were observed in WT mice (Fig. 6F).

No difference in stress-induced corticosterone secretion was detected between WT and CerS2 null mice (not shown). In contrast, evaluation of medullary function, ascertained by measuring urinary levels of epinephrine (E), norepinephrine (NE), metanephrine (MN) and normetanephrine (NMN) demonstrated that NE and NMN were elevated in 3 month-old CerS2 null mouse urine, while MN and E were elevated at 7 and 10 months of age (Fig. 6). This finding correlates with, and may precede the morphological abnormalities observed in the medulla of CerS2 null mouse adrenal gland at a later age.

Discussion

The main finding of the current study is that CerS2 null mice display a high incidence of PCC, which is preceded by medullary hyperplasia. A number of genes have been associated with the development of PCC in humans, such as the SDH gene (mitochondrial complex II subunits), the RET proto-oncogene, the von Hippel-Lindau (VHL) tumor suppressor gene or the neurofibromin 1 (NF1) gene (Fishbein & Nathanson 2012; Shah *et al.* 2012). Mutations in VHL and SDH result in accumulation of succinate which directly inhibits prolyl hydroxylase (PHD), thereby inducing Hif-1α accumulation (Favier & Gimenez-Roqueplo 2010); Hif-1α causes PCC tumorogenesis by increasing angiogenesis, proliferation, invasion and metastasis (Favier & Gimenez-Roqueplo 2010). Mutations in the RET proto-oncogene and in NF1 activate RAS/RAF/MAPK and PI3K/Akt/mTOR signaling pathways, which play critical roles in tumorogenesis (Shah *et al.* 2012).

The mechanism responsible for PCC in CerS2 null mice is not known, but is clearly related to the changes in the SL profile. Three major changes in SL levels occur in CerS2 null mice; reduction in levels of very-long chain SLs, elevation of long-chain SLs and elevation of sphinganine (and sphingosine), although the pathways by which the latter two are altered is not known. Transcriptional up-regulation of either CerS1 or CerS5/6 cannot account for increased C18- and C16-ceramide; rather, it is likely that changes in levels of these lipids are related to other changes in their metabolism (such as altered rates of synthesis *versus* degradation), although little information is currently available to assess this possibility. However, some of the pathology can be explained by changes in levels of specific lipids. For instance, C16-ceramide and sphinganine both directly inhibit complex IV activity in the liver (Zigdon *et al.* 2013), which results in oxidative stress. Altered levels of sphingosine, which is known to permeabilize lysosomes and cause relocation of lysosomal enzymes to the cytosol (Kågedal *et al.* 2001), may be related to the altered cathepsin levels, which together with oxidative stress might reduce lysosome function and thus accelerate lipofuscin accumulation.

Lipofuscin accumulates in CerS2 null mice as young as 2 months of age; this is somewhat similar to the events that occur in ABCD2-deficient mice (Lu *et al.* 2007) in which

spontaneous and premature deposition of ceroid, an end-product of oxidative damage, occurs predominantly in adrenal medullary cells. Lipofuscin is normally found in senescent post-mitotic cells such as cardiac myocytes, neurons, and in the area between the zona reticularis and the medulla in adrenal glands in old age (Kurz *et al.* 2007). Thus, the CerS2 null mouse provides additional indications that oxidative stress is a key player in PCC formation, although the mechanism of oxidative stress is somewhat different inasmuch as SDH function was normal, the Hif-1α protein was not upregulated, and Akt and mTOR phosphorylation was not detected in the PCC (data not shown); moreover, ceroid accumulation is not observed in PCC caused by SDH mutations, suggesting that the mechanism of PCC formation differs between SDH mutations and that observed in the CerS null mouse. We conclude that defects in cytochrome c oxidase (mitochondrial complex IV) (Lee & Wei 2007) may be the main mechanism by which oxidative stress in generated in the CerS2 null mouse.

The relevance of our findings on altered SL levels to human PCC is currently unclear, with only one study relating to this issue, in which SMPD1, the gene which encodes for acid sphingomyelinase, was elevated in benign compared to malignant PCC (Thouënnon *et al.* 2007). There is one report of a human patient with a mutation in CerS2, in which a 27 kb *de novo* deletion in one allele of chromosome 1q21 was detected (Mosbech *et al.* 2014), although there is no evidence that this patient displays either mitochondrial dysfunction or PCC. There is, however, a relationship between altered CerS expression and cancer. Thus, increased expression of CerS2 occurs in breast cancer (Erez-Roman *et al.* 2010; Hartmann *et al.* 2012; Fan *et al.* 2013) and CerS2 may play a role in prostate cancer (Wang *et al.* 2012; Xu *et al.* 2012); moreover, ~15% of CerS2 null mice develop hepatocellular carcinoma (HCC) and most mice develop proliferative nodules (Pewzner-Jung *et al.* 2010b).

The enhanced levels of secretion of NE and MNE into the urine is consistent with data showing that these two hormones increase in PCC (Pacak 2011). Several factors are known to enhance catecholamine secretion from the medulla of the adrenal gland, including chronic hypoglycemia and increased leptin levels (Takekoshi *et al.* 2001; Shibuya *et al.* 2002), both which are observed in CerS2 null mice (Park *et al.* 2012). Leptin stimulates the hypothalamus and increases sympathetic nerve tone (Rosol *et al.* 2001). Whether these factors are also involved in PCC formation in the CerS2 null mouse is unknown, but irrespective of the precise details of the molecular mechanism, interrogating the SL pathway might pave the way for understanding the etiology of PCC formation and for development of novel potential therapeutic approaches for the treatment of PCC.

Acknowledgments

Funding

This work was supported by the Israel Science Foundation (0888/11) and by National Institutes of Health Grant GM076217. W-J Park was supported by Basic Science Research Program through the National Research Foundation of Korea (NRF) funded by the Ministry of Education, Science and Technology (NRF-2013R1A1A1076013).

We thank Dr. Hanna Mandel, Dr. Elena Dumin, Mrs. Avital Greenberg and Mrs. Anna Ziskind from Rambam Hospital in Haifa, Israel for catecholamine analysis, Drs. Alon Chen (Weizmann Institute of Science, Rehovot, Israel), Felix Beuschlein (Ludwig-Maximilians-University Munich, Germany), Karel Pacak (National Institutes of

Health, Bethesda, MD, USA) and Eystein Sverre Husebye (University of Bergen, Norway) for helpful comments, Ms. Vered Sasson for help with initial aspects of this work, and Dr. Hyejung Park for help with the ESI-MS/MS analyses. Anthony H. Futerman is the Joseph Meyerhoff Professor of Biochemistry at the Weizmann Institute of Science.

Abbreviations

SL	sphingolipid
CerS	ceramide synthase
VLC	very-long chain
LC	long chain
NE	norepinephrine
E	epinephrine
PCC	pheochromocytoma

References

Ben-David O, Pewzner-Jung Y, Brenner O, Laviad EL, Kogot-Levin A, Weissberg I, Biton IE, Pienik R, Wang E, Kelly S, et al. Encephalopathy caused by ablation of very long acyl chain ceramide synthesis may be largely due to reduced galactosylceramide levels. Journal of Biological Chemistry. 2011; 286:30022–30033. DOI: 10.1074/jbc.M111.261206 [PubMed: 21705317]

Chen A, Zorrilla E, Smith S, Rousso D, Levy C, Vaughan J, Donaldson C, Roberts A, Lee K-F, Vale W. Urocortin 2-deficient mice exhibit gender-specific alterations in circadian hypothalamus-pituitary-adrenal axis and depressive-like behavior. The Journal of Neuroscience. 2006; 26:5500–5510. DOI: 10.1523/JNEUROSCI.3955-05.2006 [PubMed: 16707802]

Erez-Roman R, Pienik R, Futerman AH. Increased ceramide synthase 2 and 6 mRNA levels in breast cancer tissues and correlation with sphingosine kinase expression. Biochemical and Biophysical Research Communications. 2010; 391:219–223. DOI: 10.1016/j.bbrc.2009.11.035 [PubMed: 19912991]

Fan S, Niu Y, Tan N, Wu Z, Wang Y, You H, Ke R, Song J, Shen Q, Wang W, et al. LASS2 enhances chemosensitivity of breast cancer by counteracting acidic tumor microenvironment through inhibiting activity of V-ATPase proton pump. Oncogene. 2013; 32:1682–1690. DOI: 10.1038/onc.2012.183 [PubMed: 22580606]

Favier J, Gimenez-Roqueplo A-P. Pheochromocytomas: the (pseudo)-hypoxia hypothesis. Best Practice & Research. Clinical Endocrinology & Metabolism. 2010; 24:957–968. DOI: 10.1016/j.beem.2010.10.004 [PubMed: 21115164]

Fishbein L, Nathanson KL. Pheochromocytoma and paraganglioma: understanding the complexities of the genetic background. Cancer Genetics. 2012; 205:1–11. DOI: 10.1016/j.cancergen.2012.01.009 [PubMed: 22429592]

Greaves P. Histopathology of preclinical toxicity studies: interpretation and relevance in drug safety evaluation. 2011

Hannun YA, Obeid LM. Principles of bioactive lipid signalling: lessons from sphingolipids. Nature Reviews. Molecular Cell Biology. 2008; 9:139–150. DOI: 10.1038/nrm2329 [PubMed: 18216770]

Hartmann D, Lucks J, Fuchs S, Schiffmann S, Schreiber Y, Ferreirós N, Merkens J, Marschalek R, Geisslinger G, Grösch S. Long chain ceramides and very long chain ceramides have opposite effects on human breast and colon cancer cell growth. The International Journal of Biochemistry & Cell Biology. 2012; 44:620–628. DOI: 10.1016/j.biocel.2011.12.019 [PubMed: 22230369]

Hayashi M. Oxidative stress in developmental brain disorders. Neuropathology. 2009; :291–8. DOI: 10.1111/j.1440-1789.2008.00888.x

Kantorovich V, Pacak K. Pheochromocytoma and Paraganglioma. In. Progress in Brain Research. 2010; :343–373. DOI: 10.1016/S0079-6123(10)82015-1 [PubMed: 20541673]

Kågedal K, Zhao M, Svensson I, Brunk UT. Sphingosine-induced apoptosis is dependent on lysosomal proteases. Biochemical Journal. 2001; 359:335–343. [PubMed: 11583579]

Keller JN, Dimayuga E, Chen Q, Thorpe J, Gee J, Ding Q. Autophagy, proteasomes, lipofuscin, and oxidative stress in the aging brain. The International Journal of Biochemistry & Cell Biology. 2004; 36:2376–2391. DOI: 10.1016/j.biocel.2004.05.003 [PubMed: 15325579]

Kurz T, Terman A, Brunk UT. Autophagy, ageing and apoptosis: the role of oxidative stress and lysosomal iron. Archives of Biochemistry and Biophysics. 2007; 462:220–230. DOI: 10.1016/j.abb.2007.01.013 [PubMed: 17306211]

Lee H-C, Wei Y-H. Oxidative stress, mitochondrial DNA mutation, and apoptosis in aging. Experimental Biology and Medicine (Maywood, NJ). 2007; 232:592–606.

Levy M, Futerman AH. Mammalian ceramide synthases. IUBMB Life. 2010; 62:347–356. DOI: 10.1002/iub.319 [PubMed: 20222015]

Lu J-F, Barron-Casella E, Deering R, Heinzer AK, Moser AB, Demesy Bentley KL, Wand GS, Mcguinness CM, Pei Z, Watkins PA, et al. The role of peroxisomal ABC transporters in the mouse adrenal gland: the loss of Abcd2 (ALDR), Not Abcd1 (ALD), causes oxidative damage. Laboratory Investigation. 2007; 87:261–272. DOI: 10.1038/labinvest.3700512 [PubMed: 17260006]

Mohr, U. International Agency for Research on Cancer. International classification of rodent tumours. IARC Scientific Publications; 1992.

Mosbech M-B, Olsen ASB, Neess D, Ben-David O, Klitten LL, Larsen J, Sabers A, Vissing J, Nielsen JE, Hasholt L, et al. Reduced ceramide synthase 2 activity causes progressive myoclonic epilepsy. Annals of Clinical and Translational Neurology. 2014; 1:88–98. DOI: 10.1002/acn3.28 [PubMed: 25356388]

Pacak K. Pheochromocytoma: A catecholamine and oxidative stress disorder. Endocrine Regulations. 2011

Park J-W, Park W-J, Futerman AH. Ceramide synthases as potential targets for therapeutic intervention in human diseases. Biochimica Biophysica Acta. 2013; doi: 10.1016/j.bbalip.2013.08.019

Park J-W, Park W-J, Kuperman Y, Boura-Halfon S, Pewzner-Jung Y, Futerman AH. Ablation of very long acyl chain sphingolipids causes hepatic insulin resistance in mice due to altered detergent-resistant membranes. Hepatology. 2012; 57:525–532. DOI: 10.1002/hep.26015 [PubMed: 22911490]

Peaston RT, Lennard TW, Lai LC. Overnight excretion of urinary catecholamines and metabolites in the detection of pheochromocytoma. Journal of Clinical Endocrinology and Metabolism. 1996; 81:1378–1384. DOI: 10.1210/jcem.81.4.8636337 [PubMed: 8636337]

Petrache I, Kamocki K, Poirier C, Pewzner-Jung Y, Laviad EL, Schweitzer KS, Van Demark M, Justice MJ, Hubbard WC, Futerman AH. Ceramide synthases expression and role of ceramide synthase-2 in the lung: insight from human lung cells and mouse models. PloS One. 2013; 8:e62968.doi: 10.1371/journal.pone.0062968 [PubMed: 23690971]

Pewzner-Jung Y, Park H, Laviad EL, Silva LC, Lahiri S, Stiban J, Erez-Roman R, Brügger B, Sachsenheimer T, Wieland F, et al. A critical role for ceramide synthase 2 in liver homeostasis: I. alterations in lipid metabolic pathways. Journal of Biological Chemistry. 2010a; 285:10902–10910. DOI: 10.1074/jbc.M109.077594 [PubMed: 20110363]

Pewzner-Jung Y, Brenner O, Braun S, Laviad EL, Ben-Dor S, Feldmesser E, Horn-Saban S, Amann-Zalcenstein D, Raanan C, Berkutzki T, et al. A critical role for ceramide synthase 2 in liver homeostasis: II. insights into molecular changes leading to hepatopathy. Journal of Biological Chemistry. 2010b; 285:10911–10923. DOI: 10.1074/jbc.M109.077610 [PubMed: 20110366]

Pewzner-Jung Y, Tavakoli Tabazavareh S, Grassme H, Becker KA, Japtok L, Steinmann J, Joseph T, Lang S, Tuemmler B, Schuchman EH, et al. Sphingoid long chain bases prevent lung infection by Pseudomonas aeruginosa. EMBO Molecular Medicine. 2014; 6:1205–1214. DOI: 10.15252/emmm.201404075 [PubMed: 25085879]

Rosol TJ, Yarrington JT, Latendresse J, Capen CC. Adrenal gland: structure, function, and mechanisms of toxicity. Toxicologic Pathology. 2001; 29:41–48. [PubMed: 11215683]

Seehafer SS, Pearce DA. You say lipofuscin, we say ceroid: defining autofluorescent storage material. Neurobiology of Aging. 2006; 27:576–588. DOI: 10.1016/j.neurobiolaging.2005.12.006 [PubMed: 16455164]

Shah U, Giubellino A, Pacak K. Pheochromocytoma: implications in tumorigenesis and the actual management. Minerva Endocrinologica. 2012; 37:141–156. [PubMed: 22691888]

Shaner RL, Allegood JC, Park H, Wang E, Kelly S, Haynes CA, Sullards MC, Merrill AH. Quantitative analysis of sphingolipids for lipidomics using triple quadrupole and quadrupole linear ion trap mass spectrometers. Journal of Lipid Research. 2009; 50:1692–1707. DOI: 10.1194/jlr.D800051-JLR200 [PubMed: 19036716]

Shibuya I, Utsunomiya K, Toyohira Y, Ueno S, Tsutsui M, Cheah TB, Ueta Y, Izumi F, Yanagihara N. Regulation of catecholamine synthesis by leptin. Annals of the New York Academy of Sciences. 2002; 971:522–527. [PubMed: 12438173]

Sitte N, Huber M, Grune T, Ladhoff A, Doecke WD, Zglinicki Von T, Davies KJ. Proteasome inhibition by lipofuscin/ceroid during postmitotic aging of fibroblasts. FASEB Journal. 2000; 14:1490–1498. [PubMed: 10928983]

Sucheston ME, Cannon MS. Development of zonular patterns in the human adrenal gland. Journal of Morphology. 1968; 126:477–491. DOI: 10.1002/jmor.1051260408 [PubMed: 5716437]

Sullards MC, Liu Y, Chen Y, Merrill AH. Analysis of mammalian sphingolipids by liquid chromatography tandem mass spectrometry (LC-MS/MS) and tissue imaging mass spectrometry (TIMS). Biochimica Et Biophysica Acta. 2011; 1811:838–853. DOI: 10.1016/j.bbalip.2011.06.027 [PubMed: 21749933]

Takekoshi K, Ishii K, Nanmoku T, Shibuya S, Kawakami Y, Isobe K, Nakai T. Leptin stimulates catecholamine synthesis in a PKC-dependent manner in cultured porcine adrenal medullary chromaffin cells. Endocrinology. 2001; 142:4861–4871. DOI: 10.1210/endo.142.11.8484 [PubMed: 11606454]

Terman A, Gustafsson B, Brunk UT. The lysosomal-mitochondrial axis theory of postmitotic aging and cell death. Chemico-Biological Interactions. 2006; 163:29–37. DOI: 10.1016/j.cbi.2006.04.013 [PubMed: 16737690]

Thouënnon E, Elkahloun AG, Guillemot J, Gimenez-Roqueplo A-P, Bertherat J, Pierre A, Ghzili H, Grumolato L, Muresan M, Klein M, et al. Identification of potential gene markers and insights into the pathophysiology of pheochromocytoma malignancy. Journal of Clinical Endocrinology and Metabolism. 2007; 92:4865–4872. DOI: 10.1210/jc.2007-1253 [PubMed: 17878247]

Vitner EB, Dekel H, Zigdon H, Shachar T, Farfel-Becker T, Eilam R, Karlsson S, Futerman AH. Altered expression and distribution of cathepsins in neuronopathic forms of Gaucher disease and in other sphingolipidoses. Human Molecular Genetics. 2010; 19:3583–3590. DOI: 10.1093/hmg/ddq273 [PubMed: 20616152]

Wang H, Wang J, Zuo Y, Ding M, Yan R, Yang D, Ke C. Expression and prognostic significance of a new tumor metastasis suppressor gene LASS2 in human bladder carcinoma. Medical Oncology). 2012; 29:1921–1927. DOI: 10.1007/s12032-011-0026-6 [PubMed: 21755371]

Weglicki WB, Reichel W, Nair PP. Accumulation of lipofuscin-like pigment in the rat adrenal gland as a function of vitamin E deficiency. Journal of Gerontology. 1968; 23:469–475. [PubMed: 5723481]

Xu X, You J, Pei F. Silencing of a novel tumor metastasis suppressor gene LASS2/TMSG1 promotes invasion of prostate cancer cell in vitro through increase of vacuolar ATPase activity. Journal of Cellular Biochemistry. 2012

Zigdon H, Kogot-Levin A, Park J-W, Goldschmidt R, Kelly S, Merrill AH, Scherz A, Pewzner-Jung Y, Saada A, Futerman AH. Ablation of ceramide synthase 2 causes chronic oxidative stress due to disruption of the mitochondrial respiratory chain. Journal of Biological Chemistry. 2013; 288:4947–4956. DOI: 10.1074/jbc.M112.402719 [PubMed: 23283968]

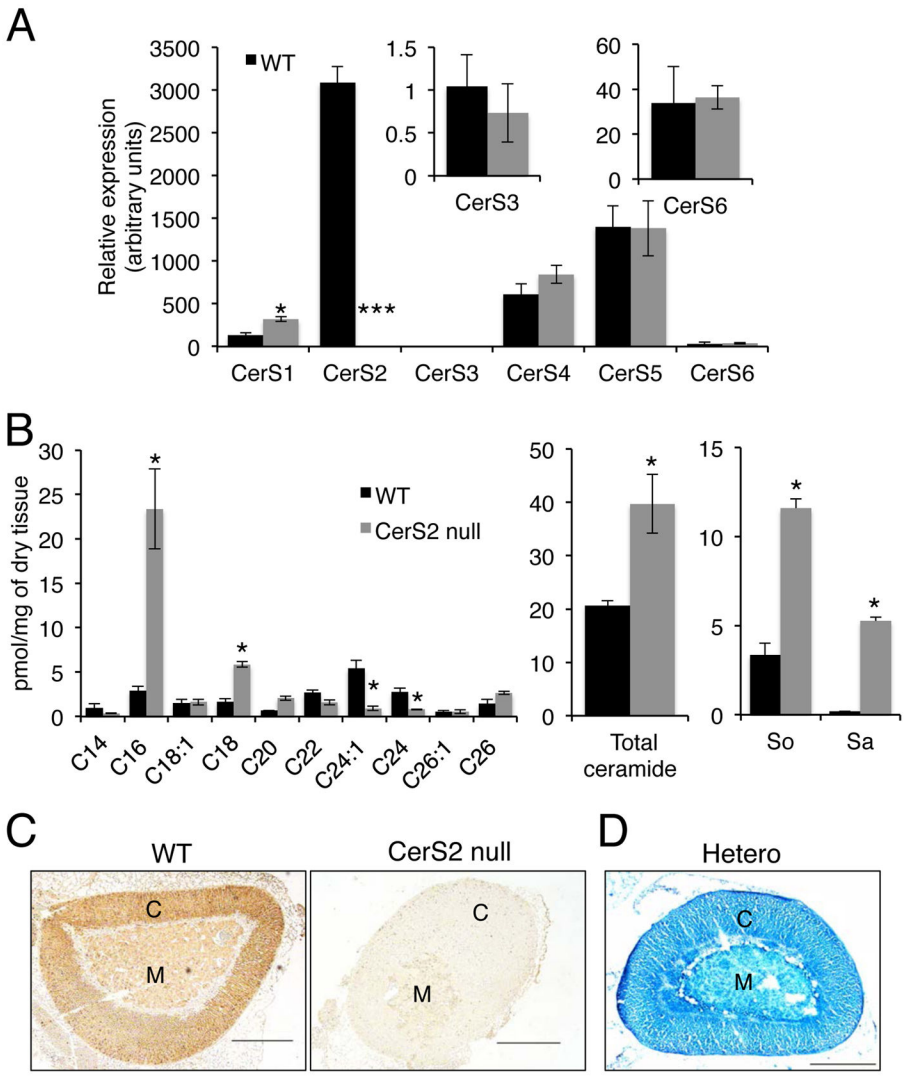

Figure 1.

CerS2 is expressed at high levels in the adrenal gland. (A) Relative CerS mRNA levels in 2-month-old WT and CerS2 null mouse adrenal gland. Data are mean ± S.E.M., n=3. **P* < 0.05, *** *P* < 0.001. (B) Ceramide and long chain base composition. The *left-hand* panel shows the acyl chain composition of ceramide, the *middle* panel levels of total ceramide and the *right-hand* panel levels of sphingosine (So) and sphinganine (Sa) in 4-month-old mice. Data are means ± S.E.M., n=2. *p< 0.05. (C) Immunostaining using an anti-CerS2 antibody in 2-month-old female mouse adrenal gland. Scale bar, 500 μm. C, cortex; M, medulla. (D) X-gal staining on cryo-sections of adrenal gland isolated from 3-month-old female CerS2 heterozygous mice. C, cortex; M, medulla. Scale bar, 500 μm.

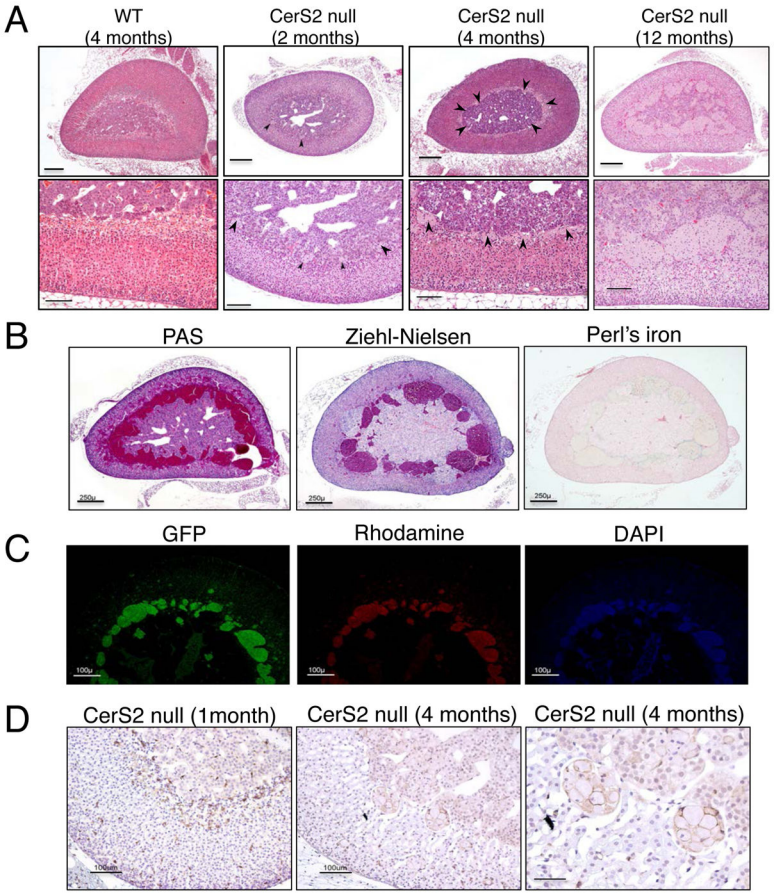

Figure 2.

Ceroid accumulation in CerS2 null mouse adrenal gland. (A) Hematoxylin and eosin staining. Arrowheads indicate ceroid accumulation in the X-zone. Scale bar, 250 μm (*upper panels*), 100 μm (*lower panels*). (B–C) Ceroid accumulation in the X-zone of the adrenal gland of 2–4 month-old male and female CerS2 null mice. Ceroid is PAS-positive, acid fast (Ziehl-Nielsen stain) and negative for iron (Perl's iron stain) scale bars, 250μm (B),100 μm (C). (D) F4/80 staining of macrophages in adrenal gland of CerS 2 null mice at 1 and 4 months of age. Arrowheads are aggregates of macrophages which are found in the X-zone between the medulla and the cortex. The *right-hand* panel is an enlargement of the middle panel. Scale bar 25 μm.

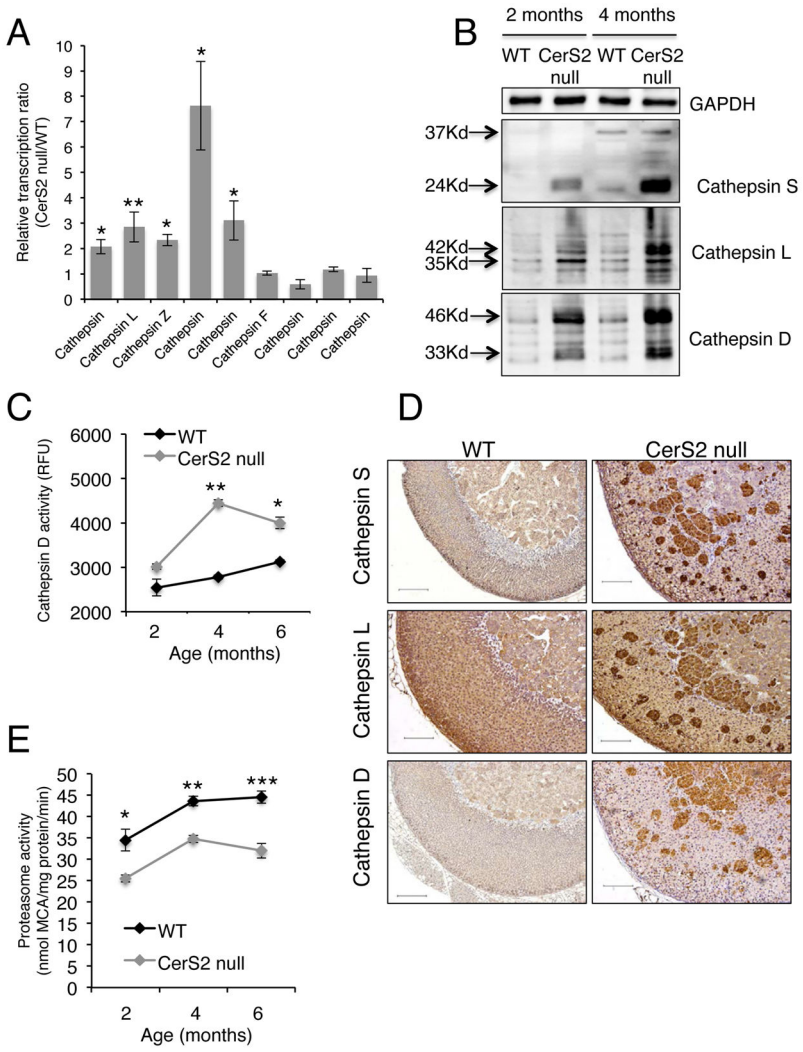

Figure 3.

Lysosomal enzyme overexpression and decreased proteasome activity. (A) Relative mRNA levels of cathepsins in the adrenal gland of CerS2 null mice. n=3; data are means ± S.E.M. *$P < 0.05$, **$P < 0.01$. (B) Representative western blot of cathepsins L, S and D in 2–4 month-old WT and CerS2 null mouse adrenal gland. GAPDH was used as loading control. (C) Activity of cathepsin D in 2, 4, and 6 month-old adrenal gland homogenates. n=3; data are means ± S.E.M. *$P < 0.05$, **$P < 0.01$. (D) Immunohistochemical staining of 4 month-old WT and CerS2 null adrenal gland using anti-cathepsin S, L and D antibodies. Scale bar, 50 μm. (E) 20S proteasome activity of WT and CerS2 null adrenal gland in 2,4 and 6 month-old adrenal gland homogenates. n=3. Data are means ± S.E.M. *$P < 0.05$, **$P < 0.01$, ***$P < 0.001$.

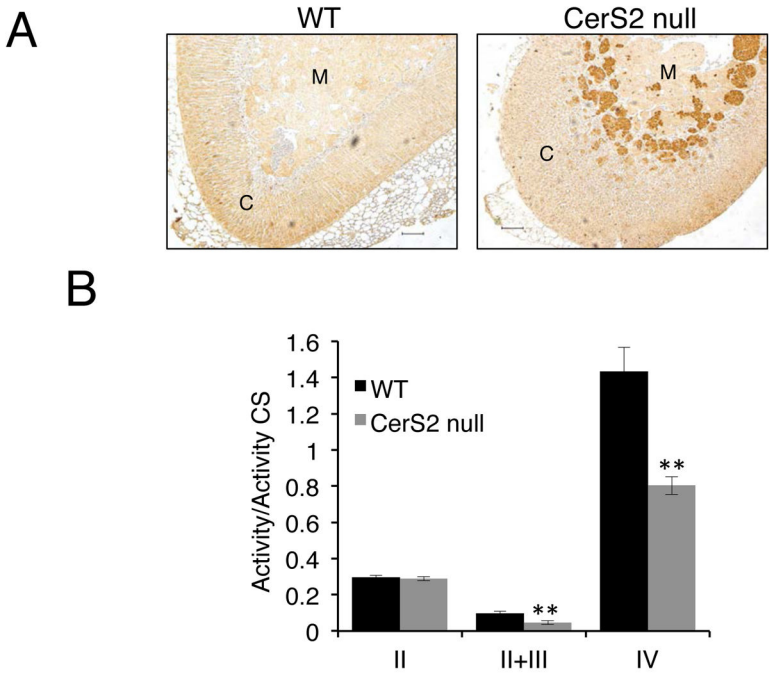

Figure 4.

Oxidative stress in CerS2 null mouse adrenal gland. (A) HNE staining in 4 month-old mice. C, cortex, M, medulla. Scale bar, 100 μm. (B) Activity of mitochondrial respiratory complexes (II, II+III, and IV), normalized to citrate synthase (CS) in 6 month-old adrenal glands (n=3). Data are means ± S.E.M. $^{**}P < 0.01$.

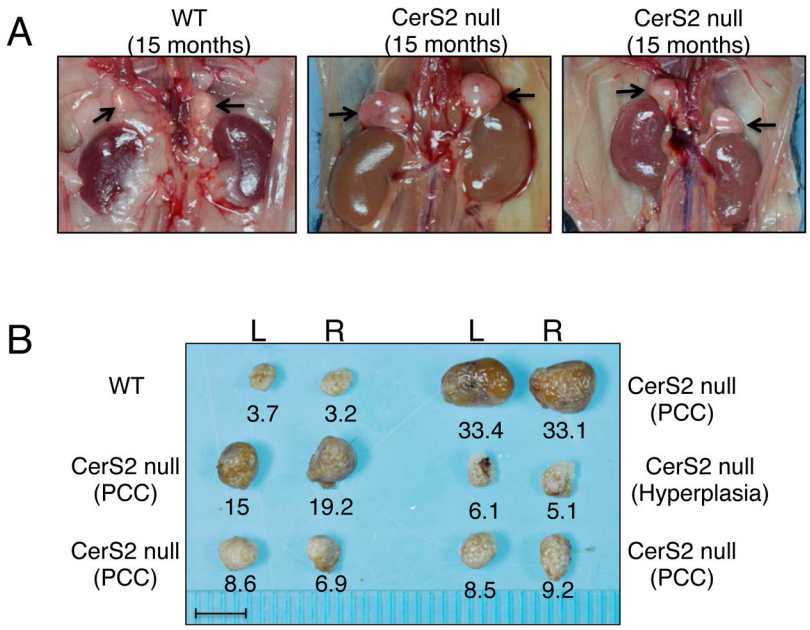

Figure 5.

Macroscopic examination of PCC in CerS2 null mice. (A) Enlarged adrenal glands (black arrows) are observed in 15-month-old CerS2 null mice. (B) CerS2 null adrenal glands. The weight of the left (L) and right (R) adrenal gland (mg) of each mouse is given beneath each image. Scale bar, 5mm.

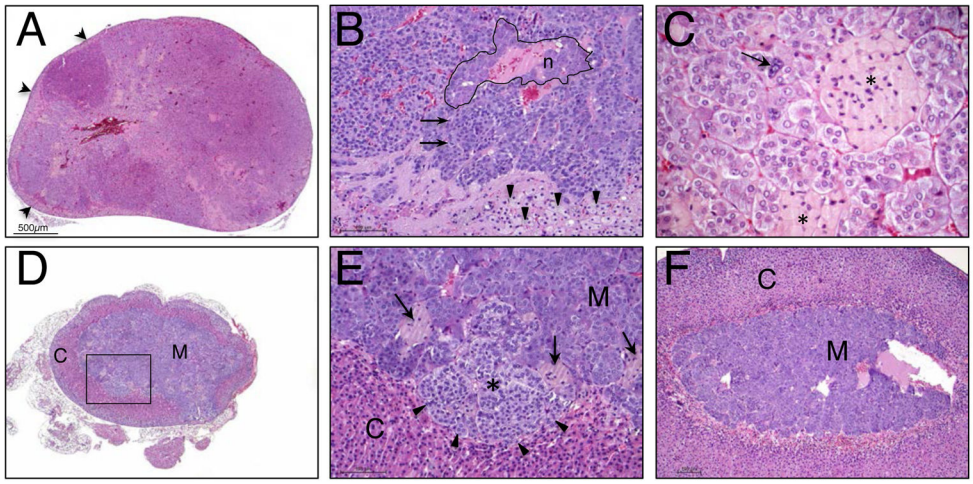

Figure 6.

Microscopic analysis of PCC in CerS2 null mice. (A) Low magnification (4x) of a PCC in the adrenal gland of a 15 month-old CerS2 null mouse. (B) Medium magnification (20x) of a typical area at the edge of a complex pheochromocytoma. Neoplastic medullary cells occupy the top 3/4 of the field. Note the higher nuclear:cytoplasmic ratio of medullary (chromaffin) cells on the left *versus* the right. Arrows point to 2 mitotic figures in the transformed population. A group of neurons is delimited by a black line. Residual cortical cells are preserved at the bottom of the field (arrowheads). (C) High magnification (40x) of PCC. The neoplastic cells show a range of cellular and nuclear sizes (anisocytosis and anisokaryosis). A cell with a large nucleus is identified (arrow). There are clusters of ceroid-laden cells in the tumor (asterisks). (D) Low magnification (4x) of an adrenal gland from a case with medullary hyperplasia. The medulla (m) is somewhat expanded but the overall corticomeduallary architecture and ratio are relatively preserved. The boxed area is shown in E. (E) Medium magnification (20x) of the insert in panel D. A small nodule of hyperplastic medullary tissue is identified with an asterisk. Note the different appearance of chromaffin cells in the nodule; the cells have a higher nuclear: cytoplasmic ratio and their cytoplasm stains more lightly. The nodule causes compression of adjacent cortical cells (arrowheads). Several clusters of ceroid-laden cells are marked (arrows). (F) Medium magnification (10x) of an adrenal gland from a WT mouse. The cortex (C) and medulla (M) are defined.

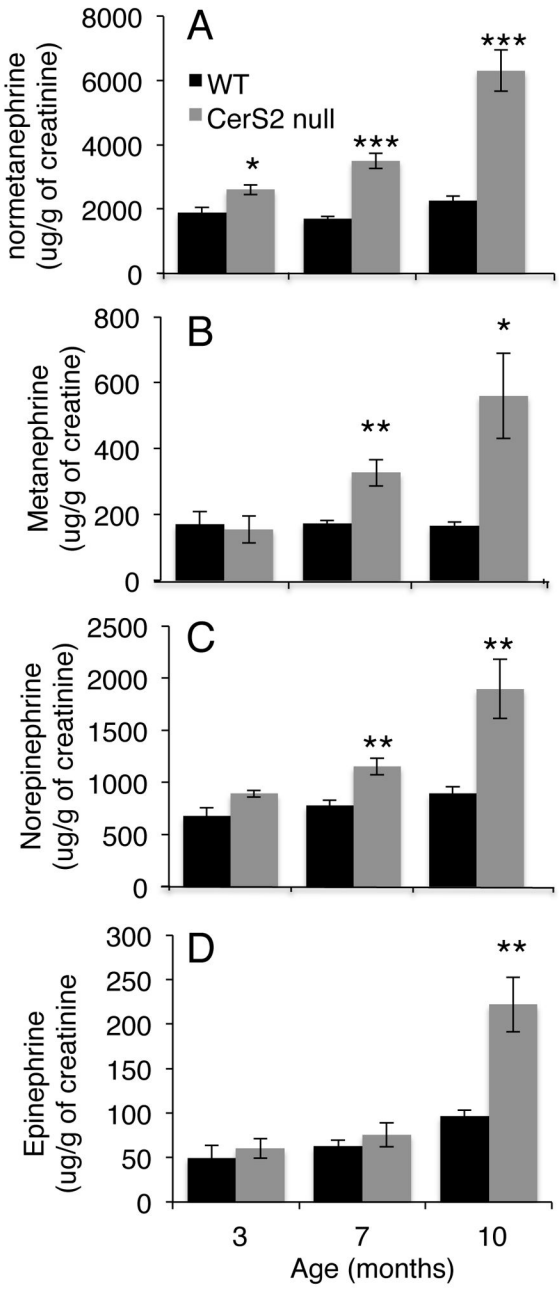

Figure 7.

Catecholamine levels are increased in the urine of CerS2 null mice. Levels of (A) normetanephrine, (B) metanephrine, (C) norepinephrine and (D) epinephrine in 3, 7 and 10 month-old WT and CerS2 null mouse urine (n=4–7). Data are means ± S.E.M. *$P < 0.05$, **$P < 0.01$, ***$P < 0.001$.